Integration of bright color centers into arrays of silicon carbide nanopillars

Enora Vuillermet, Nicolas Bercu, Serguei Kochtcheev, Mihai Lazar

▶ **To cite this version:**

Enora Vuillermet, Nicolas Bercu, Serguei Kochtcheev, Mihai Lazar. Integration of bright color centers into arrays of silicon carbide nanopillars. 2025. hal-04878667

HAL Id: hal-04878667
https://hal.science/hal-04878667v1

Preprint submitted on 10 Jan 2025

HAL is a multi-disciplinary open access archive for the deposit and dissemination of scientific research documents, whether they are published or not. The documents may come from teaching and research institutions in France or abroad, or from public or private research centers.

L'archive ouverte pluridisciplinaire **HAL**, est destinée au dépôt et à la diffusion de documents scientifiques de niveau recherche, publiés ou non, émanant des établissements d'enseignement et de recherche français ou étrangers, des laboratoires publics ou privés.

Integration of bright color centers into arrays of silicon carbide nanopillars

E. Vuillermet,[1] N. Bercu,[2] S. Kochtcheev,[1] and M. Lazar[1]
[1)]*Light nanomaterials, nanotechnologies laboratory, CNRS UMR 7076, University of Technology of Troyes, Troyes, France*
[2)]*Light nanomaterials, nanotechnologies laboratory, CNRS UMR 7076, University Reims Champagne-Ardenne, Reims, France*

(*Electronic mail: enora.vuillermet@utt.fr)

(Dated: 29 December 2024)

Silicon carbide (SiC) is a wide-bandgap semiconductor combining mature fabrication processes with the ability to host optically active point defects, called color centers, making it ideal for quantum technologies. This study focuses on silicon vacancy defects in 4H-SiC, integrated into nanopillar arrays fabricated via ion implantation, e-beam lithography, and reactive ion etching. SiC nanopillars with a height of 1.4µm are formed and arrays with varying pillar diameters and spacings are obtained. Cathodoluminescence measurements at 80 K reveal a 2–4 times improvement in light collection efficiency from the defects compared to unstructured SiC. The cathodoluminescence intensity increases with a smaller pillar spacing and a larger diameter. These findings demonstrate the potential of SiC nanopillar arrays as scalable platforms for enhancing quantum photonic device performance.

Silicon carbide (SiC) is a wide-bandgap semiconductor that has been used for decades in power device applications[1]. The maturity of its fabrication processes has resulted in the commercialization of high-quality wafers with minimal defects[2], enabling the controlled integration of point defects within the material. This has recently driven the development of SiC as a host for bright color centers with long spin coherence times for quantum applications[3,4].

Compared to other materials, such as diamond and rare-earth-doped semiconductors, SiC offers significant advantages for quantum device fabrication due to its well-established processes, including epitaxial growth[5], doping (n and p-type)[6], and etching[7]. These make SiC an ideal candidate for developing quantum platforms and devices[8,9], such as magnetic field sensors[10], quantum computing systems[11], and single-photon sources (SPSs) integrated into electronic or CMOS devices[12]. However, due to the high refractive index of SiC compared to air (around 2.65)[13], light emitted from the color centers is predominantly reflected at the SiC/air interface, leading to the need for devices that isolate single-photon sources while increasing the intensity of light collected. Previous studies have demonstrated that integrating color centers into photonic structures, such as microdisks[14], optical cavities[15], or nanopillars[16], can achieve these objectives.

In this work, we focus on the single silicon vacancy defect (V_{Si}) in 4H-SiC, a promising quantum defect with electronic spin states that can be manipulated at room temperature (RT), exhibiting spin coherence times of approximately 100µs at RT[17] and up to 20ms at cryogenic temperatures[18]. To enhance the light collection efficiency of these color centers, we incorporate them using ion implantation into nanopillar arrays fabricated on 4H-SiC substrates. This study completes the work of S. Castelletto *et al.*[19] and M. Radulaski *et al.*[16] and ensures that the silicon vacancies are generated exclusively within the nanopillars, avoiding defect formation in the substrate between the photonic structures. Additionally, we investigate the effects of varying pillar spacings on light collection efficiency, which has not been done experimentally until now to the best of our knowledge. Using cathodoluminescence (CL) at 80 K, we demonstrate a 2-4 times improvement in the light collection from the silicon vacancies compared to an unstructured SiC substrate. These results highlight the potential of SiC nanopillar arrays as a scalable platform for quantum photonic applications.

Fabrication. The nanopillars are fabricated on 4H-SiC n-doped substrates, first implanted with helium ions at an energy of 120 keV and a dose of $4 \times 10^{17} cm^{-2}$. SRIM-TRIM simulations[20,21] indicate that the silicon vacancies are primarily generated at a depth of 480nm (FIG.1).

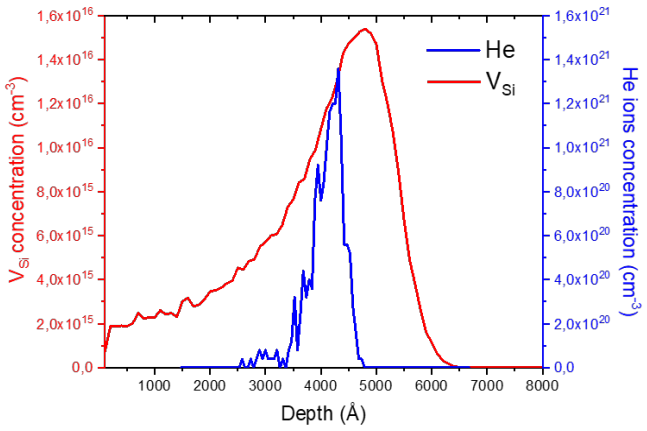

FIG. 1. SRIM-TRIM simulations depth profiles of the helium ions introduced and silicon vacancies generated during ion implantation.

One sample is kept as a reference while the other one is processed to form the nanopillar arrays. For the latter, electron beam (e-beam) lithography is performed using a Raith e-line scanning electron microscope (SEM) operating at 20keV with an aperture of 30µm and an exposure dose of 200µC/cm^2. For this step, a 450 nm-thick PMMA resist is used to pattern the samples and is developed, after e-beam exposure, into a solution of MIBK:IPA for 1min20s. Following this, a 150nm-thick chromium hard mask is deposited via electron beam evaporation at a deposition rate of 0.1nm/s using the

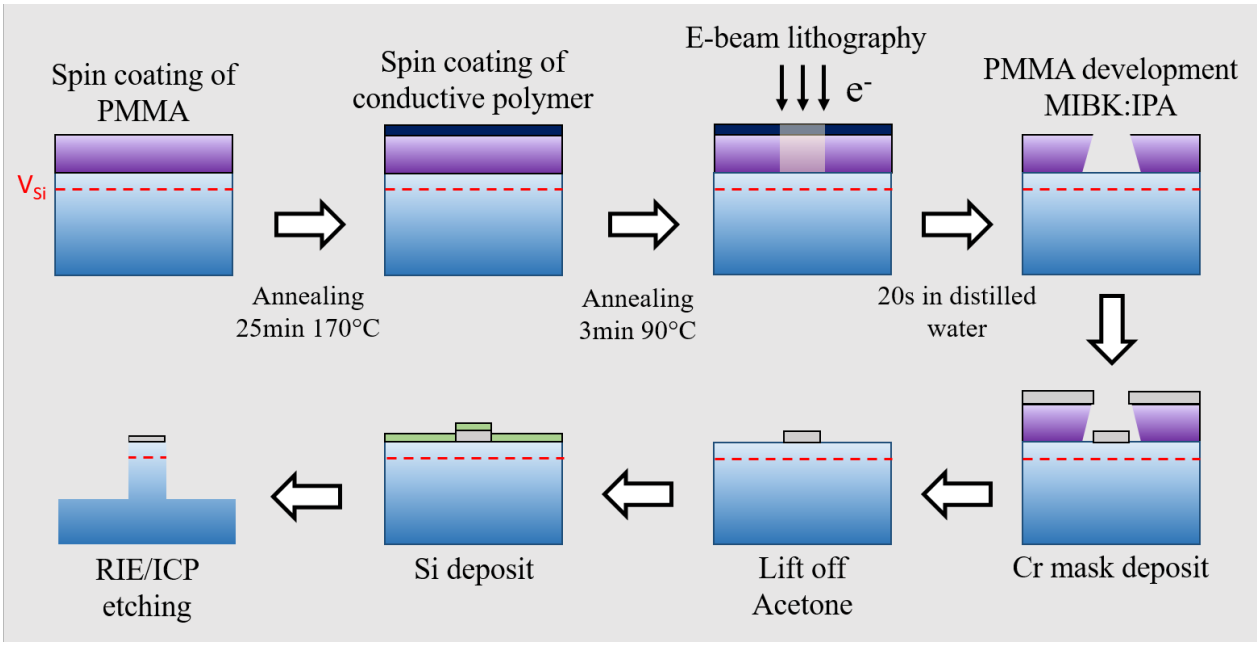

FIG. 2. Fabrication steps of the 4H-SiC nanopillars.

MEB400 system from Plassys. Lift off of the mask occurs in a solution of acetone under agitation. Reactive ion etching with inductively coupled plasma (RIE/ICP) is then carried out in a MU400 system of Plassys to form the SiC pillars. The plasma is generated at low pressure (1.067Pa) using a gas mixture of 10sccm SF_6 and 2sccm O_2, with 100W of RIE power and 1000W of ICP power. The unit "sccm" stands for Standard Cubic Centimeters per Minute. An etching speed of 4.7nm/s is achieved under a bias of -156V. To avoid micro-masking, a phenomenon where small particles or residues act as unintended masks, leading to non-uniform etching and the formation of rough uneven surfaces[22,23], a 100nm-thick silicon layer is deposited on the samples before SiC etching. After etching, the remaining chromium mask is removed using a chromium etchant solution. The plasma etching parameters were optimized through multiple experiments designed to etch SiC power devices[24]. Fabrication steps of the 4H-SiC nanopillar arrays are summarized in FIG.2. Further details are provided in the Supplementary Materials of this paper.

The resulting SiC nanopillars (FIG.3) have a height of 1.4µm, with diameters ranging from 350 to 700nm. The arrays have an area of 100×100µm^2, with pillar spacings of 336nm, 538nm, 946nm, or 5µm, as determined by the simulations presented in the paper of M.A. Ahamad *et al.*[25]. The conical shape of the chromium masks (FIG.3), combined with lateral etching during the fabrication process, contribute to a reduction in the pillar diameter (Supplementary Materials). This effect is more pronounced for arrays with larger pillar spacings (945nm and 5µm). This lateral etching, negligible during SiC power device processing, is significant in nanostructure fabrication and leads to the so-called bowing phenomenon[15,26]. Bowing refers to lateral etching or undercutting of the pillars' sidewalls, resulting in a curved or bowed profile rather than straight vertical sidewalls. Despite the pillar distortion, there is no evidence of micro-masking or trenching, thanks to the addition of the Si layer, which enhances the volatility of reaction by-products during plasma etching[23]. Trenching can be caused by ion scattering, over-etching, or charge buildup and manifests as deep, narrow grooves ("trenches") at the base or sidewalls of etched features during anisotropic plasma etching[7,27].

Cathodoluminescence measurements. Cathodoluminescence offers an alternative to photoluminescence by generating electron-hole recombination through electron beam excitation rather than laser excitation[28,29]. CL measurements are performed using a SPARC system (Delmic) integrated with a JEOL JSM-7900F SEM to identify the color centers created by ion implantation. The samples are characterized at 80K, the low temperature being maintained by a liquid nitrogen circulation system (80K Cryo-module, Kammrath and Weiss GmbH, Schwerte, Germany). A diffraction grating of 302 lines/mm with a central wavelength of 500nm is used for spectral analysis. The SEM is operated at an acceleration voltage of 15kV with a beam current of 1nA. The CL system's spectral detection range extends up to 1100nm, allowing detailed analysis of the emitted light from the silicon vacancies.

Silicon vacancies identification. Since the electron beam is focused on a precise point on the sample surface (around 1.5nm of diameter), the intensity of collected light from the V_{Si} defects varies depending on the area analyzed. FIG.4 illustrates various measurement points and their corresponding CL spectra for an array of nanopillars with a theoretical diameter of 500nm and a pillar spacing of 336nm. The typical CL

signal of the silicon vacancies appears around 900nm[30], confirming the presence of the defects within the SiC nanopillars. Because the silicon vacancy can occupy a cubic (k) or hexagonal (h) site of 4H-SiC[31], two zero-phonon lines (ZPLs), called V1 (h) and V2 (k), are observed, at 850 and 908nm respectively. The wavelengths of the ZPLs are slightly blue-shifted compared to the expected values (862nm for V1 and 917nm for V2)[32], probably due to the local strains within the 4H-SiC crystal after ion implantation. At the end, we observe that the intensity of the CL spectra is highest at the center of the pillar structures (FIG.4). Less expected, a CL signal is detected between the pillars, even with the lack of defects in this area, likely due to a resonance effect induced by the periodic array. Further measurements are thus realized with the electron beam focused at the center of the pillars.

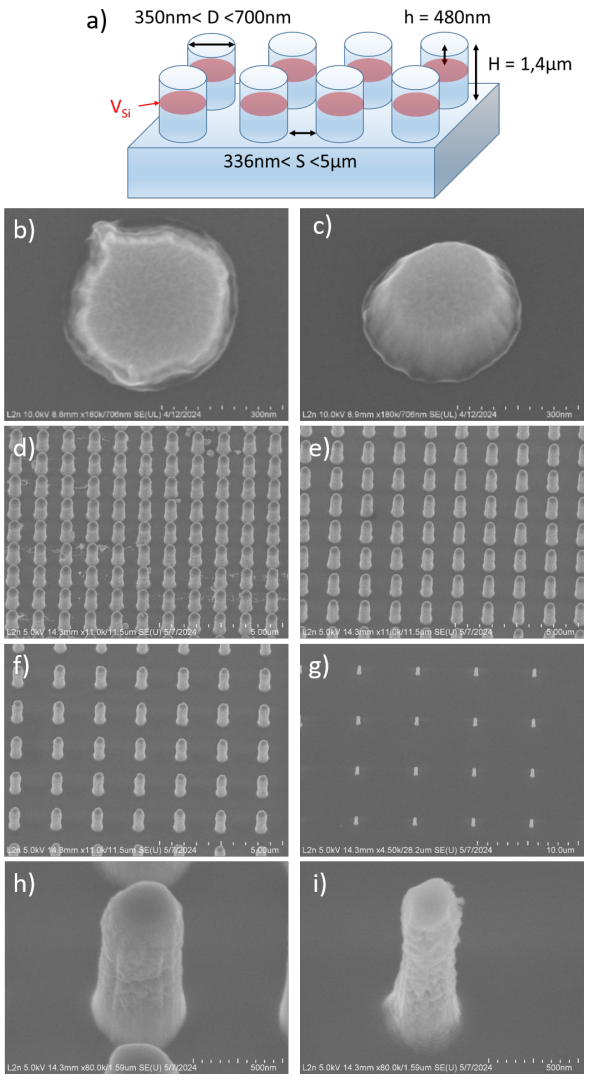

FIG. 3. Scheme of the nanopillar arrays (a) and SEM images with no tilt (b) and a 30° tilt (c) of the Cr-masks for a pillar diameter of 450nm and a spacing of 5µm. SEM images of the nanopillar arrays are also shown for a pillar diameter of 700nm and a spacing of 336nm (d), 538nm (e), 946nm (f) and 5µm (g). Images (h) and (i) are the respective zoom of images (d) and (g).

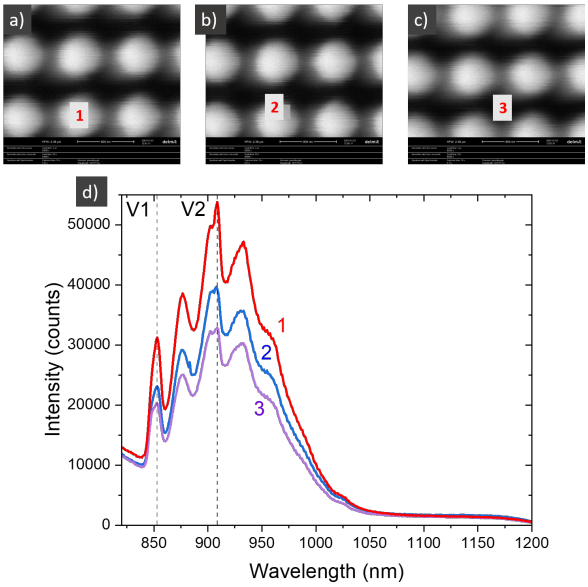

FIG. 4. SEM images under electron scanning of an array with a pillar diameter of 450nm and a spacing of 336nm (a-c). The normalized CL spectra (d) are measured at the positions 1 to 3.

Effect of arrays dimensions. As shown in FIG.5, the normalized CL spectra intensity from the V_{Si} defects increases with the pillar diameter for a given spacing between the pillars. This behavior can be attributed to a higher number of defects in larger-diameter pillars, resulting in enhanced excitation of the color centers. Unlike previous simulations and studies reported in the literature[16,19], no specific pillar diameter exhibits maximum luminescence for these defects. Additionally, the CL signal intensity increases as the pillar spacing decreases. Compared to the unprocessed reference sample, the signal is weaker in arrays with large spacings of 946nm and 5µm. This reduction is likely due to excessive lateral etching of the pillars, which distorts their vertical geometry and reduces their resonance with the silicon vacancies. In contrast, for smaller pillar spacings, particularly at 336nm, the CL intensity can double to quadruple depending on the pillar diameter compared to the reference sample without pillars. These findings confirm that the periodicity of the arrays significantly influences the intensity of light collected from the silicon vacancies. When the pillars are sufficiently close, a resonance effect occurs between the color centers and the array, enhancing the signal compared to the reference sample. Moreover, compared to previous experimental studies where the array periodicity was around 5µm[16,19], we observed a lower photon collection efficiency than the unprocessed reference sample for larger pillar spacing. This discrepancy may stem from the fact that, unlike other studies, our fabrication process included etching the SiC sample after the ion implantation step. As a result, the silicon vacancies were generated exclusively within the pillars, without any of them present in the etched surface, apart from the intrinsic defects of the 4H-SiC substrate.

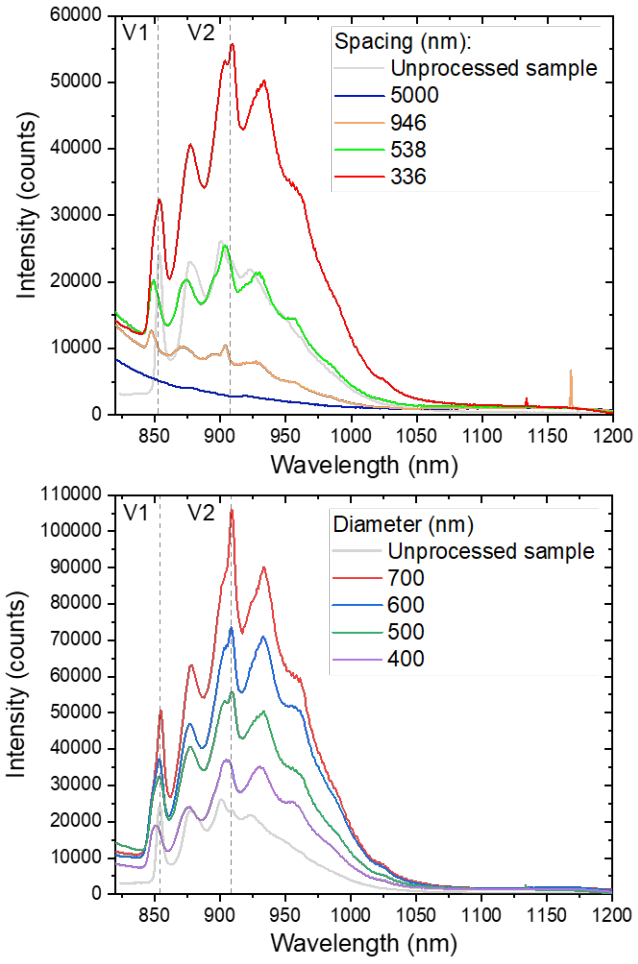

FIG. 5. CL normalized spectra of silicon vacancies for varying diameter (a) and spacings (b). The diameter is fixed at 500nm for the graphic (a) and the spacing is fixed at 336nm for the graphic (b).

This study highlights the potential of silicon carbide (SiC) nanopillar arrays as scalable and efficient platforms for enhancing light collection from color centers such as silicon vacancies in 4H-SiC. By combining color centers' generation and nanopillar fabrication, we demonstrate the compatibility of SiC with photonic structures designed for quantum applications. Due to the high applicability of ion implantation and plasma etching, this technological platform could also be adapted to integrate different color centers in other polytypes of SiC such as 3C or 6H-SiC.

While the results confirm the influence of pillar geometry and array periodicity on light collection efficiency, further work is needed to fully understand the underlying mechanisms. Numerical simulations could provide valuable insights into the role of array resonance in enhancing the light collection of the color centers. Additionally, experiments with isolated single V_{Si} defects are essential to confirm single-photon emission properties and assess the platform's potential for quantum technologies. Exploring arrays with even smaller spacings near 336nm would also help elucidate how the CL signal evolves as the pillars approach each other, potentially unlocking new regimes of photonic interaction. Finally, improvements in fabrication processes to minimize SiC lateral etching and preserve pillar integrity could further enhance device performance.

In conclusion, this work establishes a foundation for integrating quantum defects in SiC with photonic structures, paving the way for applications in quantum sensing, single-photon sources, and scalable quantum photonic devices. Future studies addressing the above challenges will bring us closer to realizing the full potential of SiC for quantum technologies.

SUPPLEMENTARY MATERIALS

This part details the fabrication steps of the 4H-SiC nanopillar arrays and the evolution of lateral etching with pillars diameters and spacings.

ACKNOWLEDGMENTS

Samples were implanted in the IP2I institute at Lyon in France. The authors acknowledge the use of resources from the Nanomat platform, part of the RENATECH network, supported by the Ministère de l'Enseignement Supérieur et de la Recherche, the Région Grand Est, and FEDER funds from the European Community. This work was made within the context of the graduate school NANO-PHOT - ANR-18-EURE-0013.

AUTHOR DECLARATION

Conflict of interest

The authors have no conflicts to disclose.

Authors contributions

E. Vuillermet: Conceptualization; Formal analysis; Investigation; Methodology; Validation; Writing – original draft. **S. Kochtcheev**: Investigation; Methodology. **N. Bercu**: Investigation; Methodology. **M. Lazar**: Conceptualization; Funding acquisition; Supervision; Validation; Writing – review and editing.

DATA AVAILABILITY STATEMENT

The data that support the findings of this study are available from the corresponding author upon reasonable request.

REFERENCES

[1] X. She, A. Q. Huang, O. Lucia, and B. Ozpineci, "Review of silicon carbide power devices and their applications," IEEE Transactions on Industrial Electronics **64**, 8193–8205 (2017).

[2] H. Matsunami, "Fundamental research on semiconductor sic and its applications to power electronics," Proceedings of the Japan Academy, Series B **96**, 235–254 (2020).

[3] S. Castelletto and A. Boretti, "Silicon carbide color centers for quantum applications," Journal of Physics: Photonics **2**, 022001 (2020).

[4] A. S. Al Atem, *Ingénierie des centres colorés dans SiC pour la photonique et la solotronique*, Ph.D. thesis, Université de Lyon (2018).

[5] T. Kimoto, "Bulk and epitaxial growth of silicon carbide," Progress in Crystal Growth and Characterization of Materials **62**, 329–351 (2016).

[6] D. Chaussende and N. Ohtani, "Silicon carbide," Single crystals of electronic materials , 129–179 (2019).

[7] K. Racka-Szmidt, B. Stonio, J. Żelazko, M. Filipiak, and M. Sochacki, "A review: Inductively coupled plasma reactive ion etching of silicon carbide," Materials **15**, 123 (2021).

[8] V. A. Norman, S. Majety, Z. Wang, W. H. Casey, N. Curro, and M. Radulaski, "Novel color center platforms enabling fundamental scientific discovery," InfoMat **3**, 869–890 (2021).

[9] M. E. Bathen and L. Vines, "Manipulating single-photon emission from point defects in diamond and silicon carbide," Advanced Quantum Technologies **4**, 2100003 (2021).

[10] S. Castelletto, C. Lew, W.-X. Lin, and J.-S. Xu, "Quantum systems in silicon carbide for sensing applications," Reports on Progress in Physics (2023).

[11] K. Khazen and H. J. von Bardeleben, "Nv-centers in sic: A solution for quantum computing technology?" Frontiers in Quantum Science and Technology **2**, 1115039 (2023).

[12] Y. Yamazaki, Y. Chiba, T. Makino, S.-I. Sato, N. Yamada, T. Satoh, Y. Hijikata, K. Kojima, S.-Y. Lee, and T. Ohshima, "Electrically controllable position-controlled color centers created in sic pn junction diode by proton beam writing," Journal of Materials Research **33**, 3355–3361 (2018).

[13] S. Rao, E. D. Mallemace, G. Faggio, M. Iodice, G. Messina, and F. G. Della Corte, "Experimental characterization of the thermo-optic coefficient vs. temperature for 4h-sic and gan semiconductors at the wavelength of 632 nm," Scientific Reports **13**, 10205 (2023).

[14] D. M. Lukin, M. A. Guidry, J. Yang, M. Ghezellou, S. Deb Mishra, H. Abe, T. Ohshima, J. Ul-Hassan, and J. Vučković, "Two-emitter multimode cavity quantum electrodynamics in thin-film silicon carbide photonics," Physical Review X **13**, 011005 (2023).

[15] D. O. Bracher and E. L. Hu, "Fabrication of high-q nanobeam photonic crystals in epitaxially grown 4h-sic," Nano letters **15**, 6202–6207 (2015).

[16] M. Radulaski, M. Widmann, M. Niethammer, J. L. Zhang, S.-Y. Lee, T. Rendler, K. G. Lagoudakis, N. T. Son, E. Janzen, T. Ohshima, *et al.*, "Scalable quantum photonics with single color centers in silicon carbide," Nano letters **17**, 1782–1786 (2017).

[17] M. Widmann, S.-Y. Lee, T. Rendler, N. T. Son, H. Fedder, S. Paik, L.-P. Yang, N. Zhao, S. Yang, I. Booker, *et al.*, "Coherent control of single spins in silicon carbide at room temperature," Nature materials **14**, 164–168 (2015).

[18] D. Simin, H. Kraus, A. Sperlich, T. Ohshima, G. Astakhov, and V. Dyakonov, "Locking of electron spin coherence above 20 ms in natural silicon carbide," Physical Review B **95**, 161201 (2017).

[19] S. Castelletto, A. S. Al Atem, F. A. Inam, H. J. von Bardeleben, S. Hameau, A. F. Almutairi, G. Guillot, S.-i. Sato, A. Boretti, and J. M. Bluet, "Deterministic placement of ultra-bright near-infrared color centers in arrays of silicon carbide micropillars," Beilstein Journal of Nanotechnology **10**, 2383–2395 (2019).

[20] V. Shulga, "Simulation of ion beam sputtering with oksana and srim: A comparative study," Vacuum **230**, 113644 (2024).

[21] I. Strašík and M. Pavlovič, "Improvements to the srim simulations," Radiation Effects & Defects in Solids **164**, 470–476 (2009).

[22] L. Voss, K. Ip, S. Pearton, R. Shul, M. Overberg, A. Baca, C. Sanchez, J. Stevens, M. Martinez, M. Armendariz, *et al.*, "Sic via fabrication for wide-band-gap high electron mobility transistor/microwave monolithic integrated circuit devices," Journal of Vacuum Science & Technology B: Microelectronics and Nanometer Structures Processing, Measurement, and Phenomena **26**, 487–494 (2008).

[23] M. Lazar, F. Enoch, F. Laariedh, D. Planson, and P. Brosselard, "Influence of the masking material and geometry on the 4h-sic rie etched surface state," in *Materials Science Forum*, Vol. 679 (Trans Tech Publ, 2011) pp. 477–480.

[24] M. Lazar, H. Vang, P. Brosselard, C. Raynaud, P. Cremillieu, J.-L. Leclercq, A. Descamps, S. Scharnholz, and D. Planson, "Deep sic etching with rie," Superlattices and microstructures **40**, 388–392 (2006).

[25] M. A. Ahamad, N. Ahmed, S. Castelletto, and F. A. Inam, "Silicon carbide pillar lattice for controlling the spontaneous emission of embedded color centers," Journal of Lightwave Technology (2023).

[26] K. Zekentes, J. Pezoldt, and V. Veliadis, "Plasma etching of silicon carbide," Mater. Res. Found **69**, 175–232 (2020).

[27] F. Simescu, D. Coiffard, M. Lazar, P. Brosselard, D. Planson, *et al.*, "Study of trenching formation during sf6/o2 reactive ion etching of 4h-sic," Journal of optoelectronics and advanced materials **12**, 766–769 (2010).

[28] B. Sieber, "Cathodoluminescence-principes physiques et systèmes de détection," (2012).

[29] A. Kakanakova-Georgieva, R. Yakimova, A. Henry, M. K. Linnarsson, M. Syväjärvi, and E. Janzén, "Cathodoluminescence identification of donor–acceptor related emissions in as-grown 4h–sic layers," Journal of applied physics **91**, 2890–2895 (2002).

[30] E. Vuillermet, N. Bercu, F. Etienne, and M. Lazar, "Cathodoluminescence characterization of point defects generated through ion implantations in 4h-sic," Coatings **13**, 992 (2023).

[31] F. A. Inam and S. Castelletto, "Metal-dielectric nanopillar antenna-resonators for efficient collected photon rate from silicon carbide color centers," Nanomaterials **13**, 195 (2023).

[32] M. Wagner, B. Magnusson, W. Chen, E. Janzén, E. Sörman, C. Hallin, and J. Lindström, "Electronic structure of the neutral silicon vacancy in 4 h and 6 h sic," Physical Review B **62**, 16555 (2000).

[33] J. Choi, L. Latu-Romain, E. Bano, F. Dhalluin, T. Chevolleau, and T. Baron, "Fabrication of sic nanopillars by inductively coupled sf6/o2 plasma etching," Journal of Physics D: Applied Physics **45**, 235204 (2012).